JAAS

ROYAL SOCIETY OF CHEMISTRY

PAPER

View Article Online
View Journal | View Issue

Cite this: *J. Anal. At. Spectrom.*, 2024, **39**, 1482

Single particle analysis of polydisperse metal-bearing particles in cannabis vape liquids by organic mode ICP-MS

Zuzana Gajdosechova * and Joshua Marleau-Gillette

The popularity of vaping cannabis-derived concentrates has grown rapidly since its legalization in several countries around the world. There is some limited evidence that metal-bearing nanoparticles (NPs) may be present in cannabis vape liquids. However, owing to the complexity of the cannabis vape liquids matrix, data on particle number concentration and particle size distribution are not available. Single particle inductively coupled plasma mass spectrometry (ICP-MS) is a technique widely used to obtain this information for samples in aqueous suspension; however, cannabis vape liquids are not water soluble. Additionally, this technique has not been well tested on naturally formed polydisperse nanoparticles, such as those found in cannabis vape liquids. An approach based on single particle analysis in organic mode ICP-MS is proposed for assessing particle number concentration and particle size distribution in cannabis vape liquids. Three approaches for determining transport efficiency were assessed, and particle sedimentation under various conditions was studied. Finally, cannabis vape liquids from nine cartridges were analyzed for several metal-bearing particles (Fe, Ni, Al, Co, Cu, Cr, V, Zn, Pb, and Sn). All samples contained a substantial number of NPs, with three samples having a number of particles one to two orders of magnitude higher than the rest of the studied samples, and the particle size distribution was, in most instances, below 150 nm for all metals.

Received 5th February 2024
Accepted 10th April 2024

DOI: 10.1039/d4ja00045e

rsc.li/jaas

Introduction

The legalization of cannabis for medical and/or recreational use has led to the development of a large variety of cannabis products delivering tetrahydrocannabinol (THC) and other cannabinoids through different entry routes. These can include inhalation (joints, vape cartridges, concentrates/distillates), ingestion (beverages, edibles, capsules, tinctures) or topical (creams and oils). Among this large number of products, cannabis vape liquids are particularly popular, as it is perceived to be a healthier alternative to traditional cannabis smoking while still providing a fast and efficient delivery of THC. Cannabis vape liquids typically consist primarily of cannabis extract, but may also include carrier solvents, flavoring agents, stabilizers, thickeners, and diluents.[1–5] These products are manufactured under various extraction techniques of *Cannabis sativa*, reduced to a distillate, blended with additives, and ultimately assembled into the final consumer product.[6–9] Due to the wide range of cannabinoid content, flavors, and additives, these concentrate products can vary significantly in pH, viscosity, and homogeneity.[10–14]

Although regulations in countries where the consumption of cannabis products is legalized require testing for arsenic (As), cadmium (Cd), mercury (Hg), and lead (Pb), recent publications have found significant levels of other metals in tested cannabis vape liquids.[15–18] Specifically, in several tested cannabis vape liquids, cobalt (Co) and vanadium (V) were found almost 10 times, chromium (Cr) and copper (Cu) 100 times, and nickel (Ni) 1000 times over the permitted levels of elemental impurities in inhaled products established by the European Pharmacopoeia.[15] The studies reported large relative standard deviations of replicate measurements, which could be caused by several factors. Cannabis vape liquids have high viscosity; thus, poor sample homogeneity can have a significant impact on the reproducibility of the analysis. Kubachka *et al.*[16] investigated several homogenization strategies and reported a decrease in the relative standard deviation between replicates when samples were heated at 120 °C for 30–60 min and continuously stirred with a stirrer bar rather than pipette tip, a comparative stirring method. Currently, cannabis vape liquids are sold pre-filled in single-use cartridges or disposable pens, generally containing between 0.5 to 1 g of product. Similar to studies of nicotine vape liquids, there is evidence that metal contaminants are leached from the metal parts of vaping cartridges.[15] Therefore, depending on the quality of the metal components, contamination may vary significantly between samples of the same production lot. Such observations were recently reported where identical cannabis vape liquids obtained from two vaping cartridges were visually different and contained significantly

National Research Council Canada, Metrology, 1200 Montreal Rd, Ottawa, ON, K1A 0R6, Canada. E-mail: Zuzana.Gajdosechova@nrc-cnrc.gc.ca

different amounts of metals.[15] Therefore, combining mass fractions obtained from identical cannabis vape liquids, but originating from two vape cartridges, could also have a significant contribution to high relative standard deviations. Another major contributor to low reproducibility are metal particles, the presence of which was recently identified by scanning electron microscopy and laser ablation inductively coupled plasma mass spectrometry.[15] Naturally formed metal particles generally vary in size, and particles of uneven size, although homogeneously distributed within the sample matrix, will significantly impact the reproducibility of the measurement.

Metal NPs have been shown to be transported into the aerosol generated by nicotine vape devices,[19,20] and as the mechanism of inhalation of cannabis vape liquids is identical, it is very likely that users of cannabis vape liquids are also exposed to metal NPs. The exposure levels may, however, differ due to difference in the vape liquid matrices, the designs, and operation conditions of vape devices, which may have an impact on the transport efficiency of the metal particles. Inductively coupled plasma mass spectrometry operated in a single particle mode (SP-ICP-MS) is often a method of choice for analysis of metal NPs. It provides information about the elemental composition of the NPs, the particle number concentration (PNC), particle size distribution (PSD), and the mass fraction of dissolved analytes. However, in contrast to nicotine vape liquids, cannabis vape liquids are not water soluble and instead require dilution into an organic solvent. Although ICP-MS is perfectly suitable for the analysis of organic solvents, there is only a handful of publications discussing measurements of NPs in organic matrices. The earliest analyses found their applications in the petrochemical industry and included investigations of naturally formed Fe, Mo,[21] and HgS[22] NPs in petroleum hydrocarbons. An additional study by Nelson *et al.*[23] looked at the stability and accuracy of the detection of engineered Fe_3O_4 NPs dispersed in crude oil. A more recent study focused on sizing TiO_2 NPs in sunscreen products using a microdroplet injector, which minimized the organic solvent load in the plasma and increased the transport efficiency of the sample.[24] The general instrument requirements for the analysis of NPs in organic matrices include the addition of O_2 into plasma to convert the carbon-based matrix into CO_2, eliminating the deposition of soot on the interface cones. As a result of O_2 addition, the plasma temperature increases, requiring the substitution of nickel interface-cones with platinum cones. The optimization of the introduction system (*i.e.*, the liquid flow rate and nebulizer gas flow rate) plays a crucial role as it determines the amount of aerosol reaching the plasma and, therefore, the ionization and atomization characteristics of the plasma. Both the sample and nebulizer flow rates are generally decreased compared to aqueous analysis, resulting in a lower amount of solvent being introduced into the plasma and increasing the plasma residence time of the NP. Increased plasma residence time is particularly important for the analysis of NPs to ensure complete ionization and, hence, accurate size determination of large NPs. As suggested by others, the plasma residence time of particles can be further increased by adjusting the plasma gas flow rate, the power for plasma generation, inner diameter of the injector and sampling position in the plasma.[25]

The aim of this study was to characterize metal particles present in widely available cannabis vape liquids purchased from the Canadian legal market. In the process, an investigation was conducted into the suitability of various methods (dynamic mass flow and size method using ligand transfer, and sequential dilution of the reference material (RM)) for the determination of NP transport efficiency, a crucial parameter for accurate sizing of NPs. Additionally, we assessed and compared the sedimentation of several reference materials in organic solvent and highlighted the possible implications this may have on PNC. Finally, the optimized method was applied to the analysis of nine cannabis vape liquids and python-based open-source SPCal software was used for data interpretation of NPs containing ten different metals.

Materials and methods

Chemicals and standards

All chemicals used were trace-metal grade quality and used without further purification. Conostan S-21 multi-elemental standard (100 mg kg^{-1}), PremiSolv solvent and HU-1 (used oil) RMs were purchased from SCP Science (Canada), dodecanethiol (DDT) and propylene glycol monomethyl ether (PGME, ≥99%) from Millipore-Sigma (Canada) and toluene and trichloromethane from Fisher Scientific (Canada). Citrate-stabilized 60 nm silver (Ag) nanoparticles (BioPure™, 59 ± 6 nm, 1 mg mL^{-1}) and polystyrene coated 100 nm gold (Au) NPs (NanoXact™, 95 ± 13 nm, 1 mg mL^{-1}) in toluene were obtained from NanoComposix (USA). Standard solution of Au (1000 mg kg^{-1}) in hydrocarbon oil was purchased from LGC (UK) and NIST SRM 1634c (trace elements in fuel oil) from National Institute of Standards and Technology (USA). Prefilled cannabis vape cartridges were purchased from the Ontario Cannabis Store (Canada).

Cannabis samples

Ten prefilled cannabis vape cartridges (Table 1) were analyzed within 2 weeks of their purchase (13-Oct-2023). The cannabis vape liquids were collected from their respective unused sealed cartridges into 2 mL Eppendorf vials following a previously described method.[15] Before sub-sampling, the cannabis vape liquids were heated for 60 min at 120 °C and continuously stirred with a stirrer bar. The sample, accurately weighed within 0.5–1 g, was diluted in 15 mL of PremiSolv and sonicated in an ultrasonic bath (Fisherbrand CPX2800 Fisher Scientific, Canada) until it was analyzed.

Reference materials

A portion of the citrate-stabilized 60 nm Ag NPs reference material was diluted to a particle concentration of approximately 2.0×10^9 particles per L *via* PGME into PremiSolv. Between each dilution, the sample was sonicated for 10 min to ensure the dispersion of NPs.

Table 1 Available information on the cannabis vape products purchased for the analysis. Mass fractions of THC and CBD compounds are reported in mg g^{-1}. All masses and mass fractions reported are based on the information provided on the packaging

Sample ID	Packaging date	Mass (g)	Δ9-THC	Total THC	CBD	Total CBD	Additional information
1	31-Mar-2023	1	825	825	2	2	Glass housing and ceramic core 510 thread cartridge
2	29-Aug-2023	1	766	809	<10	<10	510 thread cartridge
3	03-Jul-2023	1.2	770.0	770.0	12.5	12.5	510 thread cartridge
4	18-Sep-2023	1	763.5	763.5	0.0	0.0	Terpinolene 5.8%; ocimene 1.5%; limonene 0.9%, 510 thread cartridge with metal components coated in black paint
5	03-Jul-2023	1	320.548	723.117	0	<6	Total terpenes 9.077%: myrcene, pinene, limonene, 510 thread cartridge with metal components coated in white paint
6	05-Jun-2023	1	850	850	<6.0	<6.0	Pax cartridge
7	07-Jun-2023	1	810	810	3.4	3.4	510 thread cartridge
8	28-Aug-2023	1.2	833.3	833.3	<6.0	<6.0	6% terpenes: terpinolene, myrcene, ocimene, limonene, caryophyllene, 510 thread cartridge
9	08-Oct-2023	1	866	900	<2.5	<2.5	510 thread cartridge with glass inner channel
10	11-Aug-2023	0.5	858	858	2.5	2.5	Disposable vape pen

Another portion of the citrate-stabilized 60 nm Ag NPs reference material was transferred into toluene through a ligand and solvent transfer reaction, as described elsewhere.[26] Briefly, 1 mL of Ag NPs was added to 1 mL of 10 mM DDT in trichloromethane, followed by the addition of approximately 5 mL of acetone to form a single-phase solution. Subsequently, the solution was shaken for 30 s and centrifuged at 12 000*g* for 2 min to sediment DDT-capped NPs. The sedimented NPs were washed twice with ethanol/trichloromethane (5 : 1 v/v) before being dispersed in toluene by 30 s of shaking and 5 min of sonication.

Instrumentation

An 8900 ICP-MS/MS (Agilent Technologies, Santa Clara, CA, USA) equipped with a platinum sampling and skimmer cone, a MiraMist concentric nebulizer, a quartz spray chamber, and a quartz torch with 1 mm injector was used in this study. The analyses were performed in time-resolved analysis (fast TRA) mode, using a dwell time of 0.1 ms per point with no settling time between measurements. The flow rate was measured at the start and end of each sequence and was typically in the range of 0.19–0.20 mL min^{-1}. Optimization for suitable sensitivity was performed daily using a custom-made tune solution. The instrument was operated in MS/MS mode using NH_3 gas (3.0 mL min^{-1}, 30%) to detect ^{52}Cr, ^{59}Co, ^{63}Cu, ^{66}Zn, ^{107}Ag, ^{118}Sn, ^{197}Au, and ^{206}Pb, all detected on mass. Oxygen (0.38 mL min^{-1}, 25%) was used as a reaction gas for the detection of ^{27}Al (on mass), ^{51}V (mass shift to m/z 67), and ^{60}Ni (on mass). More detailed instrument settings are listed in Table 2. An Agilent SPS 4 autosampler (Agilent Technologies, Santa Clara, CA, USA) was used for sample introduction. The raw data were exported and processed with the SPCal software (version 1.1.11)[27] using automatic threshold selection with 5-sigma criteria. All graphs shown were created using OriginPro 2016 (OriginLab, Northampton, MA, USA).

Quantitation was performed using a multi-level external calibration method, and transport efficiency (also called nebulization efficiency) was compared among two methods. Firstly, using particle size method dilution of citrate-stabilized Ag NPs into PremiSolv *via* PGME or from the size of DDT-capped Ag NPs. Secondly, by using dynamic mass flow (DMF) described elsewhere.[28] Briefly, a container with PremiSolv was placed on an analytical balance with both the sample and waste tube immersed in the container and allowed to equilibrate for 30 min. The mass change (*i.e.*, the mass flow of sample reaching the plasma) was monitored for 60 min, and the change in the mass was recorded every 10 min. The recorded weights of the mass reaching the plasma were plotted against the time at which the weight was recorded (slope 1). To determine the mass flow of the sample uptake, the waste tubing was removed from the container and allowed to equilibrate for 30 min. The sample uptake was monitored for 15 min, and the mass change was recorded every 5 min. The recorded weights of the sample uptake were plotted against the time at which the weight was

Table 2 Operating conditions for the analysis of organic solvents

Tune mode	NH_3	O_2
Scan mode	MS/MS	
RF power (W)	1500	
Sampling depth (mm)	10	
Nebulizer gas (L min^{-1})	0.8	0.6
Option gas: O_2 (L min^{-1})	0.3 (30%)	
Spray chamber temp (°C)	5	
He flow (mL min^{-1})	1.0	—
NH_3 flow (mL min^{-1})	3.0 (30%)	—
O_2 flow (mL min^{-1})	—	0.38 (25%)
Octopole bias (V)	−7.5	−3.0
Axial acceleration (V)	2.00	2.0
Energy discrimination (V)	−7.2	−8.0

recorded (slope 2). The transport efficiency (η) was calculated using eqn (1):

$$\eta = \frac{\text{mass flow of sample reaching the plasma}}{\text{mass flow of sample uptake}} = \frac{\text{slope 1}}{\text{slope 2}} \quad (1)$$

Results

Quality control

To verify the accuracy of the optimized tune modes, the mass fractions of the trace metals in NIST 1634c and HU-1 were analyzed in the spectrum mode by direct dilution of the RMs in the solvent. The recoveries were within acceptable range (86–115%, $n = 3$) for all analytes of interests. During the analysis in single particle mode, two RMs (100 nm Au and 60 nm Ag) were used in each sequence: one for the determination of transport efficiency, the other as a quality control sample for size determination. Each measurement contained cannabis vape liquid spiked with 60 nm Ag and/or 100 nm Au RM, whose calculated size was within the confidence interval provided by the manufacturer: 58.6 ± 2.7 nm ($n = 12$) and 99.3 ± 4.0 nm ($n = 3$), respectively.

Comparison among transport efficiency determination methods

A precise determination of the aspirated fraction solution that reaches the plasma is fundamental for an accurate determination of PNC and PSD.[29,30] Such determination is generally done by aspirating a RM that was certified for particle size and/or particle number concentration. The range of NP RMs is very limited, and to the best of our knowledge, there were only two commercially available RMs in organic solvent. Therefore, an alternative approach for transport determination was investigated. The DMF method did not require the use of a RM, which was an advantage compared to traditional methods. Originally, the transport efficiency method using DMF was conducted with the spray chamber cooled to 2 °C;[28] however, condensation of the organic solvent was observed in the transfer tube between the spray chamber and the torch at this temperature, impacting the transport efficiency. A slight increase in the temperature of the spray chamber to 5 °C ensured the evacuation of the solvent without visible points of condensation. The transport efficiency calculated by the DMF method, measured on different days, ranged between 4.0% and 9.0% ($n = 4$), and each time it was higher than the RM transport efficiency. One of the principles of DMF lies in the precise measurement of the mass change over a selected time period. In the original publication, the measurement of mass reaching the plasma was performed over 45 min, whereas in the present work, this was increased to 60 min and, in one instance, to 120 min. This increase in the recording time interval aimed to improve the accuracy of the mass change, as with the low sample flow rate required for organic mode ICP-MS, the average mass of sample reaching plasma per recorded time interval (10 min) was 0.06 g. In each instance, slopes 1 and 2 showed excellent linearity ($r^2 \geq 0.99$). When examining the mass of the sample reaching plasma, a constant increase in the mass was observed at around 0.005 g per time interval, which was a considerable increase considering the average mass flow. Thus, it was possible that even with the increased spray chamber temperature, some condensation was taking place, and the evacuation of the introduction system was incomplete. A recent comparison study also noted a overestimation of the DMF method when performed in aqueous mode but using an instrument without a cooled spray chamber.[31] Similarly, Murphy *et al.* concluded that DMF method can achieve acceptable results only under very limiting conditions and the cause of the biases of DMF method remain to be explained.[32]

A ligand exchange reaction was performed to determine if the currently available NP RM in a water-based matrix could be used for organic solvent analysis. Following the ligand transfer reaction, DDT-capped 60 nm Ag NPs were dispersed in toluene and examined by transmission electron microscopy, which demonstrated the absence of aggregation and particles of a spherical shape without any substantial changes to the particle size (data not shown). The measured particle size by SP-ICP-MS was 59 ± 2 nm ($n = 7$), which was in good agreement with the size provided by the manufacturer (59 ± 6 nm). The ligand exchange reaction was not a quantitative reaction, as a visible amount of Ag coated the walls of the reaction container, so transport efficiency using this material could be calculated using only the particle size and not the particle frequency method. In comparison with the decreased polarity dilution transfer of NPs, the transport efficiency using DDT-capped Ag NPs was, on average, 0.3% lower and thus could be considered a suitable option for preparation of RMs in organic solvent to calculate transport efficiency.

Lastly, the use of citrate-stabilized 60 nm Ag NPs sequentially diluted *via* PGME into organic solvent resulted in a transport efficiency of around 3.0%, when particle size was used for the calculation. However, when particle frequency was used, the transport efficiency was significantly lower, around 1.8%, resulting in an incorrect size determination of the tested RMs. When using particle frequency for the determination of transport efficiency, the calculation was based on the accurate concentration of aspirated NPs in the solution. Clearly, the particle frequency method underestimated the transport efficiency. The transport efficiency using particle frequency method is expressed as a ratio between the number of observed particle events and the number of introduced particles in the suspension of known PNC. The accuracy of this method can be hindered by particles loss along the sample introduction pathway which could happened during addition of O_2 gas. Oxygen is being added in the elbow connector of the spray chamber which may introduce turbulence to the sample flow and hence disperse some NPs which eventually don't reach the plasma.

Sedimentation of NPs in the organic matrix

Multi-elemental analysis of NPs performed on a quadrupole ICP-MS significantly increases the analysis time, as the selected

sample acquisition time is multiplied by the number of analytes to be quantified. Due to the prolonged analysis time, sedimentation of the NPs can occur. As shown in Fig. 1a–c, when RMs were diluted and kept undisturbed for 60 min after the first analysis, significant sedimentation (*i.e.*, loss of particle number) was observed (blue line in Fig. 1a–c). Subsequent measurements, performed every 2 min, showed a random change in particle number, suggesting that the major portion of NPs sedimented within the first hour. This trend was reduced when the samples were sonicated and vortexed between the individual measurements (red line in Fig. 1a–c). Sedimentation was eliminated when 10 mM DDT was added to the diluting solvent, and the samples were sonicated and vortexed between analyses. Reduced sedimentation of TiO_2 NPs dispersed in toluene containing 10 mM DDT had been previously reported.[24] When no DDT was used, sedimentation of TiO_2 NPs (approximately 60–70%) was observed over 12 min, whereas the addition of 10 mM DDT resulted in reduced sedimentation (approximately 15%). However, the authors did not report sonication or vortexing of the samples before measurement, which may have eliminated the sedimentation as observed in the present study. The time interval of 60 min for sedimentation in the present study was selected according to the duration of the calibration sequence. For calibration purposes, a multi-point and multi-elemental calibration was performed, requiring 60 min; consequently, the RM was measured 60 min after the start of the sequence.

Although the addition of 10 mM DDT in combination with sonication and vortexing appeared to be an ideal condition for the analysis, the addition of 10 mM DDT into the cannabis vape liquid resulted in phase separation. Cannabis vape liquids contain a large number of organic complexes that may be sensitive to the polarity of the matrix. Therefore, the cannabis vape liquids were diluted in the organic solvent without DDT. The diluted sample was placed into the autosampler, and measurement of Co and Sn NPs were recorded every 5 min for a duration of 25 min, which was the total time required for the analysis of one sample. As seen in Fig. 1d., the sedimentation trend varied significantly between the two studied analytes. Cobalt NPs exhibited sedimentation over the studied time interval, whereas Sn NPs displayed a random change in the detected particle number.

NPs analysis in cannabis vape liquids

Ten different cannabis vape liquids in unused cartridges were selected for analysis based on the different designs of the

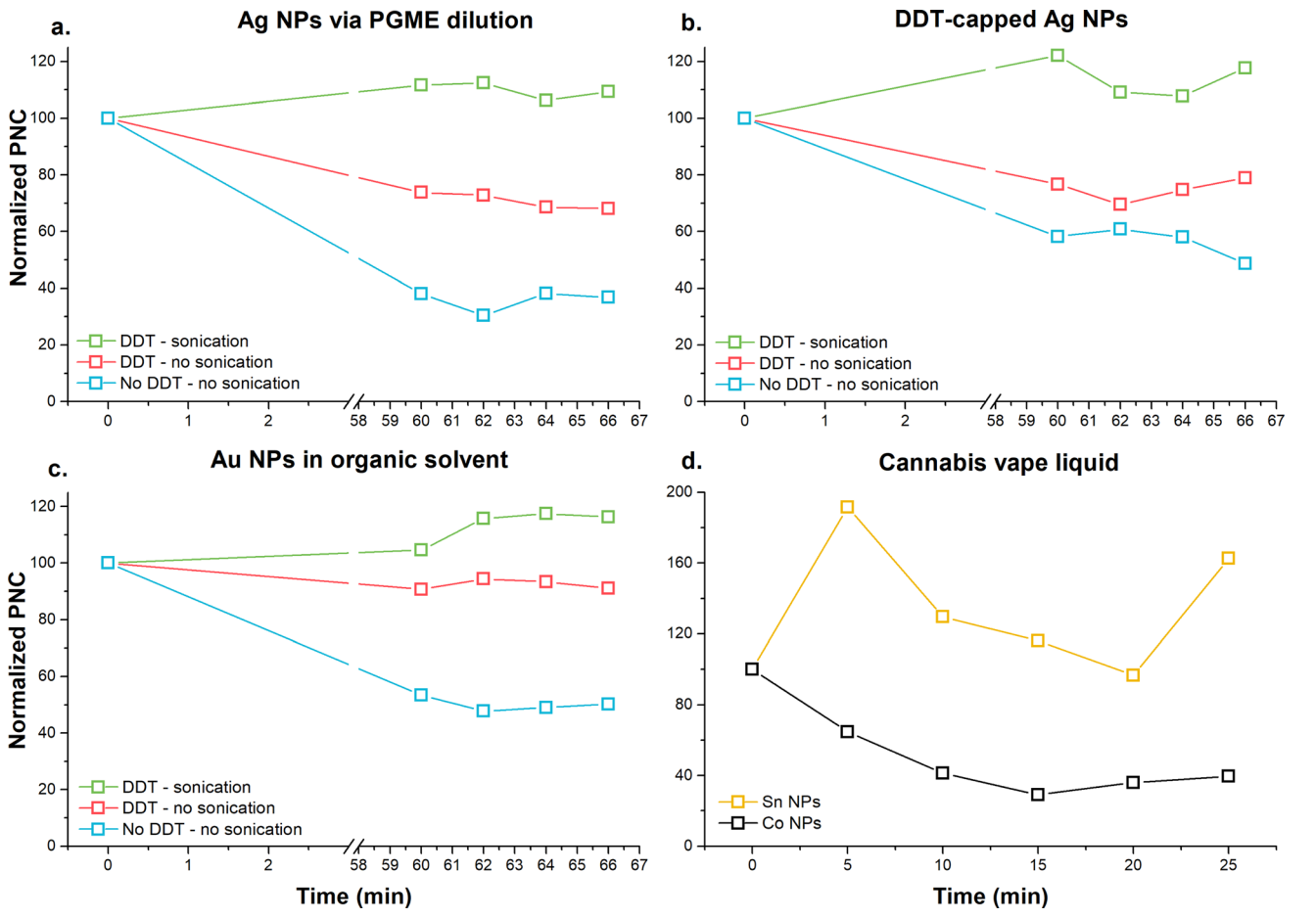

Fig. 1 Sedimentation trends of (a) Ag RM in organic solvent *via* PGME dilution, (b) Ag RM in organic solvent prepared *via* ligand exchange, (c) Au RM in organic solvent diluted from toluene, and (d) Co and Sn NPs in the cannabis vape liquids under studied experimental conditions.

atomizers in which they were contained. After the transfer from the atomizers, visible precipitates were observed at the bottom of the Eppendorf vial in four samples. Sample 6 contained dark brown flakes resembling fibres, which turned into precipitate after heating and diluting in the organic solvent. Due to the visible precipitate in the diluted solution, sample 6 was excluded from the analysis to avoid blockage of the introduction system. Instead, sample 6 was centrifuged to facilitate NP sedimentation and the sample matrix was used for spiking with RMs to assess the matrix effect on the NP sizing. Precipitates were also found in an additional three samples (samples 4, 5, and 8), but upon heating and diluting in the organic solvent, they dissolved. Initially, all samples were diluted approximately 13-fold; however, samples 5 and 9 had to be further diluted by 200-fold and sample 8 by 1000-fold due to the large number of particles present in these samples.

All samples were analyzed for NPs containing ten elements (Fe, Ni, Al, V, Cu, Co, Zn, Cr, Pb, and Sn), which were found to be present in most of the samples. Wash samples containing only the diluent (organic solvent) were measured between each cannabis sample to monitor NP carry-over. Most of the wash samples contained, on average, ≤20 NPs of selected analytes, with the exception of Cu, which had an average count of 77 NPs, Fe with an average count of 233 NPs, and Al with an average count of 245 NPs. Unfortunately, Fe and Al NPs seemed to be present in the diluent, as a similar average count of these NPs was detected throughout the entire work with this solvent.

It should be noted that some samples contained a large number of metal particles whose signal distribution appeared as if these samples contained several distinct sizes of NPs. Fig. 2a shows the signal distribution of Cu in sample 8, which was diluted 13-fold. The signal distribution could be interpreted as corresponding to NPs of several distinct sizes; however, after additional dilution (100-fold), the signal distribution changed to one typically observed for samples containing polydisperse NPs (Fig. 2b). However, the detected particle number did not correspond to the dilution factor applied. The number of particles detected in the 13-fold diluted sample 8 was calculated as 8133, but after 100-fold dilution, the number of particles decreased only slightly to 7388. Clearly, not all particles have been counted in the 13-fold diluted sample.

In an ideal system, the particle number should decrease linearly with an increased dilution factor. However, in polydisperse samples, such as samples with naturally formed NPs, this non-linear decrease in PNC may be caused by several factors. Firstly, with high PNC, there is a very large probability of multiple particle events, which will result in the underestimation of the PNC and overestimation of the PSD. Thus, when the sample is being diluted, the number of multiple particle events is reduced, and hence the PNC doesn't follow a linear decrease. Secondly, with the introduction of sample dilution, the mass fraction of dissolved analyte is diluted, resulting in a lower particle detection threshold. Consequently, smaller particles become detectable and increase the PNC. Therefore, several dilution factors should be tested when analyzing polydisperse NP samples as it was previously suggested by others.[33,34]

NPs present in cannabis vape liquids are naturally formed, most likely as a result of corrosion or thermal expansion and cooling-induced degradation, such as chipping or cracking of the metal components. Due to the size heterogeneity of the NPs and the possible presence of dissolved ionic fractions of the studied analytes, assigning the signal produced by NPs and dissolved analytes was quite challenging. As seen in Fig. 3, there was a distinct drop in the frequency of signal distribution between dissolved and particulate Ag when the RM was analyzed, known as the particle detection threshold (Fig. 3a), which was absent in the real samples with a heterogeneous size distribution (Fig. 3b).

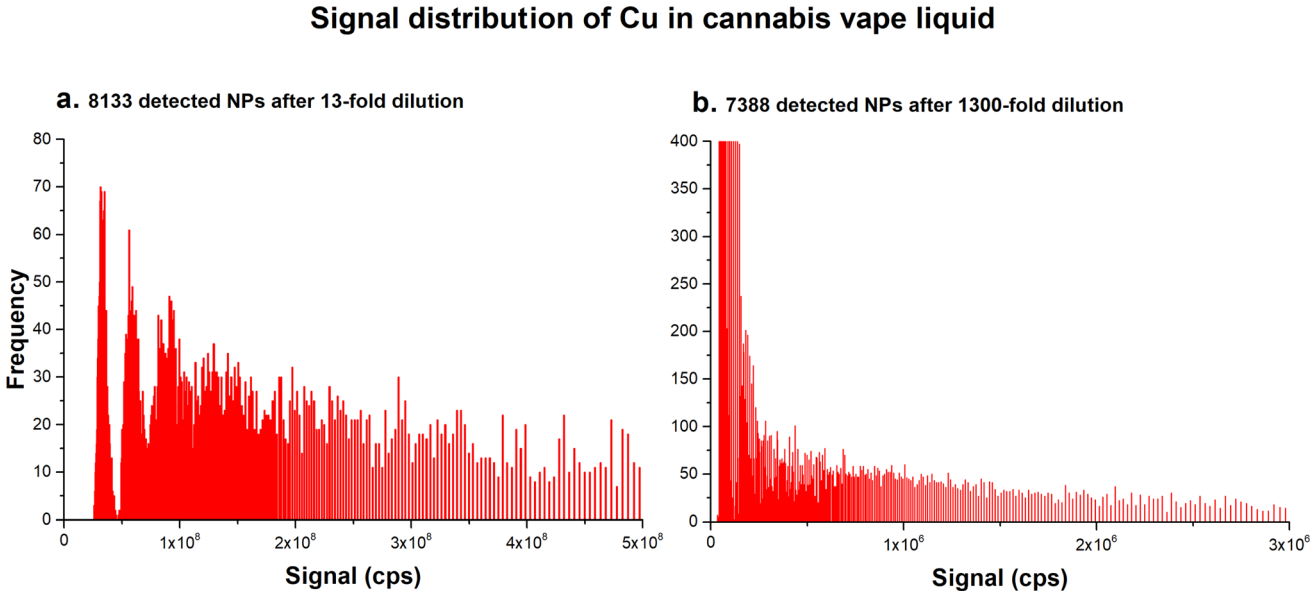

Fig. 2 Signal distribution of Cu detected in sample 8 (a) after a 13-fold dilution, and (b) after an additional 100-fold dilution.

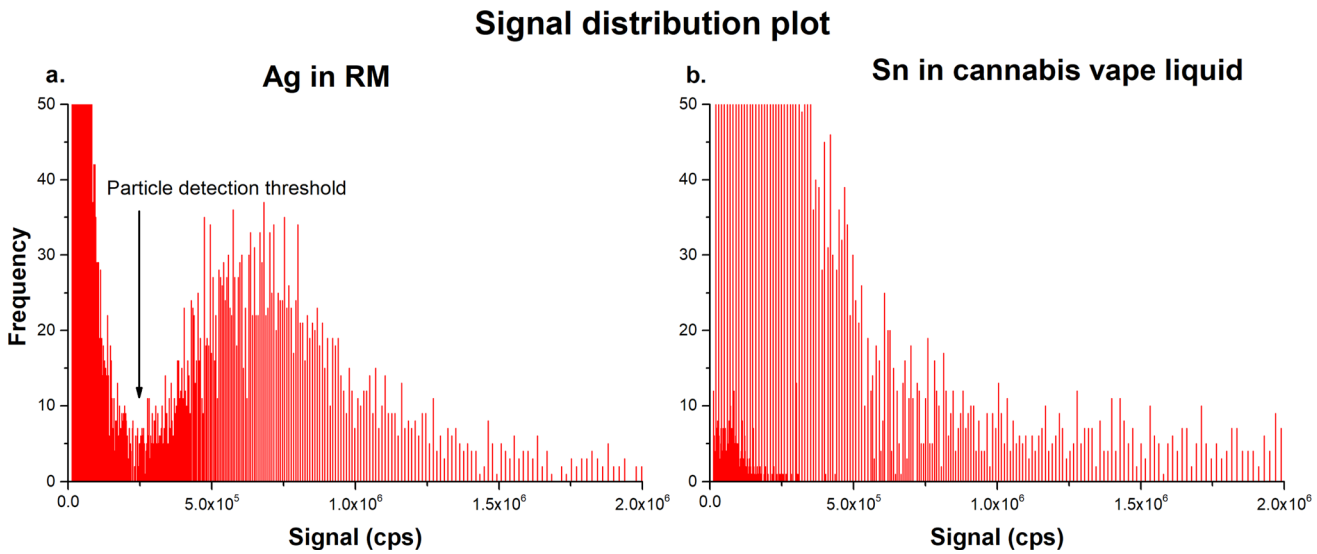

Fig. 3 Signal distribution of (a) 2837 Ag NPs in 60 nm RM, and (b) 2487 Sn NPs in cannabis vape liquid. Particle detection threshold distinguishes between signal generated by dissolved ions and NPs of a given analyte.

Although both samples contained a similar number of NPs (2837 for Ag RM and 2487 for Sn in the cannabis vape liquids), assigning the particle detection threshold in the cannabis samples was challenging based on visual examination of the signal distribution chart. The calculation of the particle detection threshold in the software provided by the instrument manufacturer was determined by the approximation of the ionic signal portion as an exponential function, as described in detail elsewhere.[35] Briefly, the signal distribution plot was constructed by integration of the raw signals, which were then counted within each period. Applying an exponential function to the data points in the signal distribution plot, plurality of approximate curves approximating the ionic signal portion was calculated. Then, the coefficient of determination (R^2) was calculated for each approximation curve, and the one with the maximum correlation was selected. Data points corresponding to the curve with the maximum correlation were selected as the particle detection threshold.

However, because the raw data are treated as a chromatographic spectrum a continuous uniform baseline has been applied, and only the signal above the baseline was integrated. This approach introduced several inaccuracies. The criterion for the baseline selection is not transparent and because the baseline is continuous over the entire acquisition time, corrections for possible signal fluctuation are not possible. More importantly, application of the uniform baseline results in the reduction of peak area and possible negative bias in counting of the small particles ultimately leading to larger size distribution and detection of fewer particles. Therefore, the raw data were processed using an open-source software SPCal,

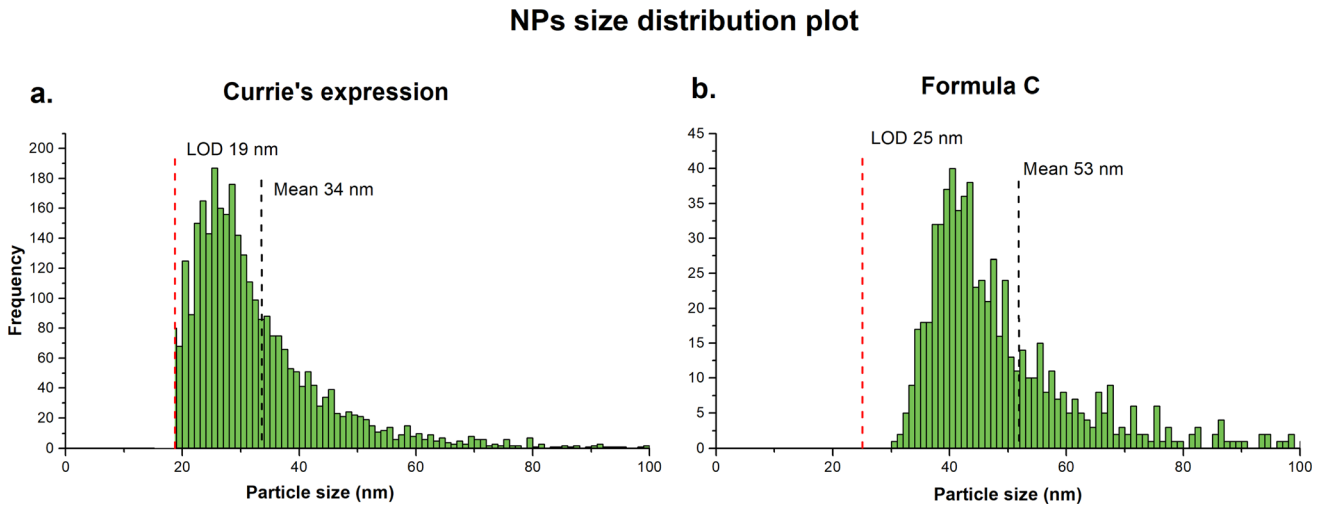

Fig. 4 Comparison of particles size distribution plots obtained by data processing using Carrie's expression (a) which counted 3191 particles and Formula C (b) which counted 696 particles.

applying iterative automatic threshold detection method. Depending on the signal intensity, the software automatically switches between Poisson filter (<50 counts) and Gaussian filter (>50 counts).[36] The critical value (L_C), defined as signal intensity that is significantly higher than the background and limit of detection (L_D) were first calculated based on selected expression for paired observations.[37] The signal above the L_D was then background-corrected and integrated to generate a single particle distribution plot. Additionally, to reduce the signal intensity contribution from dissolved ions in the sample and thus reduce the L_D, samples were sequentially diluted. The raw data in this study were processed using both Currie's expression and Formula C, and significant differences were found in the output results. When applying Currie's expression (Fig. 4a), a higher PNC was obtained (3191 particles) with a lower mean PSD (34 nm) compared to Formula C (Fig. 4b), which counted 696 particles with a mean PSD of 53 nm. Upon closer examination of the raw signal, it was observed that Formula C filtered out a larger number of data points belonging to the dissolved analyte. As a result of its higher filtration efficiency, *i.e.*, a more conservative approach, the PSD seemed to be fully distinguished from the dissolved background. On the other hand, the

Table 3 Information values for mean size, LOD and PNC of NPs bearing selected metals measured in cannabis vape liquids[a]

Analyte	Sample ID	Mean size (nm)	LOD (nm)	NPs/device	Analyte	Sample ID	Mean size (nm)	LOD (nm)	NPs/device
Fe	1	71	30	1.52×10^5	Co	1	NQ	NQ	ND
	2	NQ	NQ	NQ		2	NQ	NQ	ND
	3	103	53	6.32×10^5		3	66	28	5.32×10^5
	4	75	32	2.96×10^5		4	NQ	NQ	ND
	5	63	29	1.30×10^8		5	65	29	1.44×10^6
	7	122	67	1.98×10^6		7	NQ	NQ	ND
	8	60	27	8.37×10^7		8	83	40	3.86×10^6
	9	68	28	1.07×10^8		9	77	30	6.20×10^6
	10	96	45	3.60×10^7		10	63	36	2.76×10^7
Ni	1	NQ	NQ	NQ	Zn	1	NQ	NQ	ND
	2	NQ	NQ	NQ		2	NQ	NQ	ND
	3	110	46	6.24×10^5		3	141	68	2.29×10^6
	4	NQ	NQ	NQ		4	NQ	NQ	ND
	5	109	43	3.80×10^6		5	161	81	3.55×10^7
	7	107	43	2.28×10^5		7	179	87	2.28×10^5
	8	98	43	8.69×10^7		8	121	61	9.03×107
	9	120	51	7.61×10^6		9	181	84	5.22×10^6
	10	104	42	2.19×10^6		10	127	68	1.24×10^7
Al	1	120	47	1.12×10^5	Cr	1	NQ	NQ	ND
	2	149	67	3.17×10^5		2	87	44	4.52×10^5
	3	177	110	1.40×10^6		3	72	29	3.91×10^5
	4	135	49	2.36×10^5		4	NQ	NQ	ND
	5	76	39	1.14×10^8		5	69	30	1.50×10^6
	7	154	81	9.34×10^6		7	69	30	6.41×10^5
	8	54	26	1.74×10^8		8	76	33	6.42×10^6
	9	90	44	8.59×10^7		9	75	30	3.82×10^6
	10	98	44	5.51×10^6		10	73	29	5.00×10^5
V	1	NQ	NQ	NQ	Pb	1	NQ	NQ	NQ
	2	99	67	5.81×10^6		2	NQ	NQ	NQ
	3	NQ	NQ	NQ		3	NQ	NQ	NQ
	4	NQ	NQ	NQ		4	NQ	NQ	NQ
	5	54	29	5.49×10^5		5	NQ	NQ	NQ
	7	NQ	NQ	NQ		7	NQ	NQ	NQ
	8	59	34	6.61×10^5		8	67	33	9.35×10^5
	9	53	28	2.37×10^5		9	75	42	7.88×10^5
	10	NQ	NQ	NQ		10	ND	ND	ND
Cu	1	NQ	NQ	NQ	Sn	1	NQ	NQ	NQ
	2	NQ	NQ	NQ		2	NQ	NQ	NQ
	3	86	37	1.82×10^6		3	97	39	4.79×10^5
	4	74	31	7.37×10^4		4	NQ	NQ	NQ
	5	95	35	7.09×10^6		5	110	38	8.07×10^5
	7	103	41	2.57×10^5		7	NQ	NQ	NQ
	8	207	94	5.84×10^8		8	145	66	1.20×10^7
	9	81	34	5.57×10^6		9	110	42	2.08×10^7
	10	93	45	8.92×10^6		10	98	41	4.31×10^5

[a] NQ – not quantified due <100 detected particles per minute of acquisition time.

PSD was incomplete, limited by the LOD, when Currie's expression was applied. Based on these observations, data were processed using Formula C are reported.

As shown in Table 3, all studied samples contained metal particles. Samples 5, 8, and 9 had the highest number of particles, generally one or two orders of magnitude higher than the rest of the studied samples. Samples 8, 9, and 10 belonged to the same producer but were contained in different designs of vape devices. Samples 8 and 9 were in a vape cartridge, which was mounted by a user on a reusable battery, whereas sample 10 was packaged in a disposable pen. Additionally, the inner channel of the vape cartridge of sample 8 was coated with black paint, while the inner channel of sample 9 was made of glass. Sample 5 was produced by a different manufacturer and was contained in a cartridge of a similar design to most of the studied samples. The inner channel of the cartridge was coated in white paint. Similarly, sample 4 had the inner channel of the cartridge coated in black paint, and contrary to samples 5 and 8, the PNC was within the range of the majority studied samples. Thus, without deeper investigation into the composition of the cartridge parts, it was not feasible to explain why samples 5, 8, and 9 contained a significantly higher PNC of all studied metals. Comparison of PNC between different samples can be somewhat misleading, because the amount of dissolved analyte has a direct impact on the LOD, which affects the PNC; thus, samples with considerably different LODs may not be directly comparable.

Vanadium is rarely reported in studies of vaping devices; however, small quantities of V were previously measured in cannabis vape liquids,[15] and V NPs were detected in some of the studied samples (Table 3). The PNC below the level of quantitation was measured in majority of samples analysed for Pb particles. Samples in which <100 particles were measured within a minute of acquisition time were excluded from reporting, as 100 particle events is the minimum number concentration limit of quantitation under ideal counting conditions.[37] As mentioned previously, Al- and Fe-containing NPs were detected in the diluent; however, the PNC in the samples was >1500 particle events, whereas the blanks systematically contained <250 NPs. Therefore, Al and Fe PNCs reported in Table 3 were corrected for the average PNCs measured in the blanks; however, the PSD may be skewed by the PSD found in the blanks.

The PSD varied considerably between analytes. While the mean size of particles containing V, Co, Cr, and Pb was <100 nm in all samples, the mean size of particles containing Zn was >120 nm in all instances. The mean sizes of particles containing other metals were mostly distributed in the range of 60 to 150 nm. Similar mean sizes of metal particles were previously reported in the aerosols from nicotine vape devices,[19] where also a considerable size variation between aerosol generated from different nicotine devices was observed. However, as discussed previously, the presence of dissolved analytes in the samples may have led to an overestimation of particle size, and thus, the reported PSD and PNC in this study should be taken as an informational value only. The presence of dissolved analytes in both the sample and diluent matrix have had a direct impact on the LOD of the measured particles. For some metals such as Co, the LOD range across studied samples has shown relatively narrow variability, ranging from 28 to 44 nm. In contrast, the LOD for Al has exhibited a wider range, varying between 26 and 110 nm. Additionally, the calculated particle size is influenced by the assumption that the particles are spherical and possess a density equivalent to that of a bulk metal, which may not hold true for naturally formed composite particles.

Conclusion

The single particle ICP-MS method for detecting metal-containing NPs in cannabis vape liquids diluted in an organic solvent was scrutinized. A comparison of two methods for calculating transport efficiency revealed that the DMF method might be biased due to incomplete sample evacuation from the introduction system. Reference materials transferred to organic solvent *via* ligand exchange reaction and through dilution in PGME provided very similar transport efficiencies, making both methods suitable alternatives when RMs in organic solvents are unavailable. The investigation of NP sedimentation demonstrated that both RMs and naturally polydisperse NPs undergo sedimentation, which could be mitigated by adding organic stabilizers such as DDT, mechanical shaking, and/or sonication. Furthermore, the sedimentation of naturally formed NPs appears to be dependent on the physical and/or chemical properties of the NPs. It should also be noted that data processing platforms can have a significant impact on the reported PNC and PSD. Future publications should clearly disclose how the raw data were treated to provide meaningful comparison between published results.

The analyzed cannabis vape liquids were found to contain a large number of NPs with various metals. Three analyzed samples exhibited a particle count one or two orders of magnitude higher than the rest of the studied samples, and the particle size distribution for most metals was predominantly below 150 nm. The presence of dissolved analytes and polydisperse particles in the studied samples was evident and may have influenced the reported PNC in a negatively biased manner and the PSD in a positively biased manner. Consequently, it is advisable to consider the reported values as semi-quantitative. Moreover, although a significant number of metal-bearing particles were detected in cannabis vape liquids, it does not guarantee that all these particles can be transported into the aerosol, and further studies should be conducted to investigate the presence of NPs in aerosols.

Conflicts of interest

There are no conflicts to declare.

Acknowledgements

ZG would like to acknowledge Katrin Loeschner, Francisco Laborda and David Clases for helpful discussions and suggestions for data evaluation strategies.

References

1 I. Kosarac, *et al.*, Open Characterization of Vaping Liquids in Canada: Chemical Profiles and Trends, *Front. Chem.*, 2021, **9**(756716), 1–10.
2 J. Meehan-Atrash and I. Rahman, Cannabis Vaping: Existing and Emerging Modalities, Chemistry, and Pulmonary Toxicology, *Chem. Res. Toxicol.*, 2021, **34**, 2169–2179.
3 A. B. Stefaniak, *et al.*, Toxicology of flavoring- and cannabis-containing e-liquids used in electronic delivery systems, *Pharmacol. Ther.*, 2021, **224**, 107838.
4 A. K. Holt, J. L. Poklis and M. R. Peace, The history, evolution, and practice of cannabis and E-cigarette industries highlight necessary public health and public safety considerations, *Journal of Safety Research*, 2023, **84**, 192–203.
5 S. A. Shehata, *et al.*, Vaping, Environmental Toxicants Exposure, and Lung Cancer Risk, *Cancers*, 2023, **15**, 4525.
6 D. De Vita, *et al.*, Comparison of different methods for the extraction of cannabinoids from cannabis, *Nat. Prod. Res.*, 2019, 1.
7 L. Baldino, M. Scognamiglio and E. Reverchon, Supercritical fluid technologies applied to the extraction of compounds of industrial interest from Cannabis sativa L. and to their pharmaceutical formulations: a review, *J. Supercrit. Fluids*, 2020, **165**(104960), 1–10.
8 M. P. Lazarjani, *et al.*, Processing and extraction methods of medicinal cannabis: a narrative review, *Journal of Cannabis Research*, 2021, **3**(32), 1–15.
9 M. Szalata, *et al.*, Simple Extraction of Cannabinoids from Female Inflorescences of Hemp (Cannabis sativa L.), *Molecules*, 2022, **27**(5868), 1–18.
10 J. W. King, The relationship between cannabis/hemp use in foods and processing methodology, *Curr. Opin. Food Sci.*, 2019, **28**, 32–40.
11 F. Siano, *et al.*, Comparative Study of Chemical, Biochemical Characteristic and ATR-FTIR Analysis of Seeds, Oil and Flour of the Edible Fedora Cultivar Hemp (Cannabis sativa L.), *Molecules*, 2019, **24**(83), 1–13.
12 A. Banerjee, *et al.*, Synthesis, characterization and stress-testing of a robust Quillaja saponin stabilized oil-in-water phytocannabinoid nanoemulsion, *Journal of Cannabis Research*, 2021, **3**(43), 1–14.
13 M. Valizadehderakhshan, *et al.*, Extraction of Cannabinoids from Cannabis sativa L. (Hemp)—Review, *Agriculture*, 2021, **11**(384), 1–21.
14 S. U. K. R. Sagili, *et al.*, Effects of Particle Size, Solvent Type, and Extraction Temperature on the Extraction of Crude Cannabis Oil, Cannabinoids, and Terpenes, *ACS Food Sci. Technol.*, 2023, **3**, 1203–1215.
15 Z. Gajdosechova, *et al.*, Evidence That Metal Particles in Cannabis Vape Liquids Limit Measurement Reproducibility, *ACS Omega*, 2022, 42783–42792.
16 K. M. Kubachka and R. A. Wilson, Elemental Analysis of Tetrahydrocannabinol and Nicotine E-Liquids Related to EVALI, *ACS Omega*, 2021, **6**(47), 32090–32100.
17 T. Muthumalage, *et al.*, Chemical constituents involved in e-cigarette, or vaping product use-associated lung injury (EVALI), *Toxics*, 2020, **8**(2), 25.
18 N. Gonzalez-Jimenez, *et al.*, Analysis of toxic metals in aerosols from devices associated with electronic cigarette, or vaping, product use associated lung injury, *Toxics*, 2021, **9**(10), 240.
19 R. S. Pappas, *et al.*, Toxic metal-containing particles in aerosols from pod-type electronic cigarettes, *J. Anal. Toxicol.*, 2021, **45**(4), 337–347.
20 S. Soulet and R. A. Sussman, A critical review of recent literature on metal contents in e-cigarette aerosol, *Toxics*, 2022, **10**(9), 510.
21 J. Nelson, *et al.*, Characterization of dissolved metals and metallic nanoparticles in asphaltene solutions by single-particle inductively coupled plasma mass spectrometry, *Energy Fuels*, 2017, **31**(11), 11971–11976.
22 D. Ruhland, *et al.*, AF4-UV-MALS-ICP-MS/MS, spICP-MS, and STEM-EDX for the Characterization of Metal-Containing Nanoparticles in Gas Condensates from Petroleum Hydrocarbon Samples, *Anal. Chem.*, 2019, **91**(1), 1164–1170.
23 J. Nelson, *et al.*, Detection of iron oxide nanoparticles in petroleum hydrocarbon media by single-particle inductively coupled plasma mass spectrometry (spICP-MS), *J. Nanopart. Res.*, 2020, **22**(10), 304.
24 J. Kocic, *et al.*, Direct analysis of nanoparticles in organic solvents by ICPMS with microdroplet injection, *J. Anal. At. Spectrom.*, 2022, **37**(8), 1738–1750.
25 F. Laborda, *et al.*, Catching particles by atomic spectrometry: benefits and limitations of single particle-inductively coupled plasma mass spectrometry, *Spectrochim. Acta, Part B*, 2023, **199**, 106570.
26 R. M. Dragoman, *et al.*, Surface-Engineered Cationic Nanocrystals Stable in Biological Buffers and High Ionic Strength Solutions, *Chem. Mater.*, 2017, **29**(21), 9416–9428.
27 T. E. Lockwood, R. G. de Vega and D. Clases, An interactive Python-based data processing platform for single particle and single cell ICP-MS, *J. Anal. At. Spectrom.*, 2021, **36**(11), 2536–2544.
28 S. Cuello-Nuñez, *et al.*, The accurate determination of number concentration of inorganic nanoparticles using spICP-MS with the dynamic mass flow approach, *J. Anal. At. Spectrom.*, 2020, **35**(9), 1832–1839.
29 H. E. Pace, *et al.*, Determining transport efficiency for the purpose of counting and sizing nanoparticles via single particle inductively coupled plasma mass spectrometry, *Anal. Chem.*, 2011, **83**(24), 9361–9369.
30 H. E. Pace, *et al.*, Single particle inductively coupled plasma-mass spectrometry: a performance evaluation and method comparison in the determination of nanoparticle size, *Environ. Sci. Technol.*, 2012, **46**(22), 12272–12280.
31 O. Geiss, *et al.*, Determination of the Transport Efficiency in spICP-MS Analysis Using Conventional Sample Introduction Systems: An Interlaboratory Comparison Study, *Nanomaterials*, 2022, **12**(4), 725.
32 K. E. Murphy, *et al.*, Comparison of direct and indirect measures of transport efficiency in single particle

inductively coupled plasma mass spectrometry, *Spectrochim. Acta, Part B*, 2024, **212**, 106841.

33 A. C. Gimenez-Ingalaturre, *et al.*, How to trust size distributions obtained by single particle inductively coupled plasma mass spectrometry analysis, *Anal. Bioanal. Chem.*, 2023, **415**(11), 2101–2112.

34 S. G. Bevers, *et al.*, Improved methodology for the analysis of polydisperse engineered and natural colloids by single particle inductively coupled plasma mass spectrometry (spICP-MS), *Environ. Sci.: Nano*, 2023, **10**(11), 3136–3148.

35 T. Itagaki, S. Wilbur and M. Yamanaka, Automated detection of nanoparticles using single-particle inductively coupled plasma mass spectrometry (SP-ICP-MS), *US Pat.*, Agilent Technologies, Inc., USA, 11075066, 2021.

36 T. E. Lockwood, R. Gonzalez de Vega and D. Clases, An interactive Python-based data processing platform for single particle and single cell ICP-MS, *J. Anal. At. Spectrom.*, 2021, **36**(11), 2536–2544.

37 L. A. Currie, Limits for qualitative detection and quantitative determination. Application to radiochemistry, *Anal. Chem.*, 1968, **40**(3), 586–593.